MOLECULAR AND CELLULAR BIOLOGY, Oct. 2008, p. 6426–6438 Vol. 28, No. 20
0270-7306/08/$08.00+0 doi:10.1128/MCB.00359-08

Oct4/Sox2-Regulated miR-302 Targets Cyclin D1 in Human Embryonic Stem Cells[▽]†

Deborah A. Greer Card,[1]‡ Pratibha B. Hebbar,[1]‡ Leping Li,[2] Kevin W. Trotter,[1] Yoshihiro Komatsu,[3] Yuji Mishina,[3] and Trevor K. Archer[1]*

Chromatin and Gene Expression Section, Laboratory of Molecular Carcinogenesis,[1] Biostatistics Branch,[2] and Molecular Developmental Biology Group, Laboratory of Reproductive and Developmental Toxicology,[3] National Institute of Environmental Health Sciences, Research Triangle Park, North Carolina 27709

Received 3 March 2008/Returned for modification 21 April 2008/Accepted 8 August 2008

Oct4 and Sox2 are transcription factors required for pluripotency during early embryogenesis and for the maintenance of embryonic stem cell (ESC) identity. Functional mechanisms contributing to pluripotency are expected to be associated with genes transcriptionally activated by these factors. Here, we show that Oct4 and Sox2 bind to a conserved promoter region of miR-302, a cluster of eight microRNAs expressed specifically in ESCs and pluripotent cells. The expression of miR-302a is dependent on Oct4/Sox2 in human ESCs (hESCs), and miR-302a is expressed at the same developmental stages and in the same tissues as Oct4 during embryogenesis. miR-302a is predicted to target many cell cycle regulators, and the expression of miR-302a in primary and transformed cell lines promotes an increase in S-phase and a decrease in G_1-phase cells, reminiscent of an ESC-like cell cycle profile. Correspondingly, the inhibition of miR-302 causes hESCs to accumulate in G_1 phase. Moreover, we show that miR-302a represses the productive translation of an important G_1 regulator, cyclin D1, in hESCs. The transcriptional activation of miR-302 and the translational repression of its targets, such as cyclin D1, may provide a link between Oct4/Sox2 and cell cycle regulation in pluripotent cells.

Pluripotent stem cells preserve their identity by promoting self-renewal and preventing differentiation. Transcription factors expressed early in development play a key role in regulating these processes. The first cell fate decision in the preimplantation embryo requires Oct4, a transcription factor expressed in the blastocyst that represses differentiation in the inner cell mass (28). Oct4 works in concert with a transcription factor binding partner, Sox2, and the pair is known to activate genes essential for early development (5, 29, 32, 36, 41, 42). Upon the formation of the late blastocyst, a third factor, Nanog, is required to repress the differentiation of pluripotent cells to visceral and parietal endoderm (26), highlighting the importance of these transcription factors in maintaining pluripotency at early developmental phases. All three of these factors are also expressed in human embryonic stem cells (hESCs) and mouse ESCs (mESCs), and the transcriptional programs orchestrated by the coordinated efforts of these factors are key mechanisms of maintaining pluripotency. Recent studies of ESCs have revealed a considerable number of genomic regions with overlapping Oct4, Sox2, and Nanog binding sites adjacent to genes that are likely important for pluripotency (2, 24). Functional analysis of the genes expressed and regulated by these transcription factors will further elucidate new mechanisms associated with the maintenance of pluripotency.

Included in this candidate set of factors are microRNAs (miRNAs) (2, 24). Like Oct4, Sox2, and Nanog, miRNAs have also been implicated in the maintenance of cell fate and the regulation of stem cell differentiation. miRNAs regulate their targets posttranscriptionally by pairing with a short antisense region of the mRNA 3′-untranslated region (3′UTR) to affect its stability and/or translation. The miR-302 gene encodes a cluster of eight miRNAs (miR-302b*-b-c*-c-a*-a-d-367) that are specifically expressed in hESCs and embryonal carcinoma cells (39). The murine homolog of miR-302a was originally cloned from mESCs (15). The gene is organized such that all eight miRNAs are first expressed as a single mRNA primary transcript prior to processing and maturation by Drosha/DGCR8 and Dicer (39). Similar clusters of miRNAs are subject to transcriptional activation by transcription factors (31), are transcribed by RNA polymerase II, and contain a 5′ cap and a polyadenylated tail (4, 19).

Here, we show that Oct4, Sox2, and Nanog bind to the promoter region of the miR-302 cluster of miRNAs in hESCs and that Oct4 and Sox2 are required for the transcriptional regulation of miR-302a in these cells. When expressed in nonpluripotent primary and transformed cells, miR-302a promotes an increase in S-phase cells and a decrease in G_1-phase cells, likely due to the cumulative effects of a number of cell cycle targets. In the converse experiment, the inhibition of miR-302 in hESCs causes the number of G_1 cells to increase. Furthermore, we show that one of miR-302's predicted cell cycle targets, cyclin D1, is posttranscriptionally regulated by these miRNAs in hESCs. The transcriptional activation of miR-302

* Corresponding author. Mailing address: Chromatin and Gene Expression Section, Laboratory of Molecular Carcinogenesis, National Institute of Environmental Health Sciences, 111 Alexander Drive, MD D4-01, P.O. Box 12233, Research Triangle Park, NC 27709. Phone: (919) 316-4565. Fax: (919) 316-4566. E-mail: archer1@niehs.nih.gov.

† Supplemental material for this article may be found at http://mcb.asm.org/.

‡ These authors contributed equally to this study.

▽ Published ahead of print on 18 August 2008.

by Oct4/Sox2 may therefore be participating in the regulation of the pluripotent cell cycle.

MATERIALS AND METHODS

Plasmids. A 56-bp fragment of the wild-type (WT) cyclin D1 3′UTR containing the putative miR-302a binding site or a mutant cyclin D1 3′UTR sequence was generated by annealing the primer pairs listed in Table S2 in the supplemental material. The fragments were then cloned into the SacI and HindIII sites of the pMIR-REPORT luciferase plasmid (Ambion, Austin, TX) by using standard molecular techniques. pGL3-miR-302 was created by cloning the PCR-amplified, ~1-kb region of the miR-302 promoter into the KpnI and BglII sites of the pGL3-Basic vector (Promega, Madison, WI) by using standard molecular techniques. The PCR primer sequences for cloning the promoter fragment are listed in Table S3 in the supplemental material. The expression constructs for Oct4 (pCAG-Myc-Oct4) and Sox2 (pCAG-HA-Sox2) were obtained from Addgene (Addgene, Cambridge, MA) (30).

Cell lines, cell culture, and transfection. hESC lines H1 (WiCell, Madison, WI) and BG-01 (hESBGN-01; BresaGen, Inc., Athens, GA) were maintained on mitotically inactivated mouse embryonic fibroblasts (MEFs) in medium containing Dulbecco's modified Eagle's medium F-12 (DMEM; Invitrogen, Carlsbad, CA) supplemented with 20% knockout serum replacement (Invitrogen), 1 mM L-glutamine (Invitrogen), 0.1 mM β-mercaptoethanol, 1% nonessential amino acids (Invitrogen), and 4 ng/ml human basic fibroblast growth factor (bFGF) (Invitrogen) at 37°C and 5% CO_2. H1 cells were supplemented with fresh medium every day and were passaged once weekly by incubation with 1 mg/ml collagenase IV (Invitrogen) according to the manufacturer's instructions. BG-01 cells were maintained and passaged in the same manner. Where indicated, BG-01 cells were grown on Matrigel (BD Biosciences, San Jose, CA) supplemented with MEF-cultured medium and 4 ng/ml human bFGF. Retinoic acid (RA) (1 μM; Sigma-Aldrich, St. Louis, MO) or vehicle was added to the medium for the indicated number of days. HeLa cells (CCL-2; ATCC, Manassas, VA) and MCF-7 cells (ATCC) were grown in DMEM (Invitrogen) supplemented with 10% fetal bovine serum (HyClone, Logan, UT) under the same conditions. Normal human fibroblasts (NHFs) were grown in DMEM supplemented with 10% fetal bovine serum (7).

BG-01 hESs were transfected by nucleofection (Amaxa, Gaithersburg, MD) according to the manufacturer's instructions for mESCs, using the A23 program. For small interfering RNA (siRNA)-mediated knockdown of Oct4 and Sox2, cells were transfected with 100 nM each Oct4 and Sox2 siRNA (Santa Cruz Biotechnology, Santa Cruz, CA) or 200 nM nontargeting siRNA control number 1 (Dharmacon, Lafayette, CO). Approximately 48 h later, lysates were harvested. For nucleofection with miR-302 inhibitors (200 pmol each anti-miR-302a, anti-miR-302b, anti-miR-302c, and anti-miR-302d; Dharmacon), hESCs were transfected for 72 h. For luciferase experiments, BG-01 cells were transfected with 40 ng pRL-CMV (Promega, Madison, WI) and 100 ng WT cyclin D1 or mutant cyclin D1 vector in addition to either 25 nM each anti-miR-302a (Ambion), anti-miR-302b (Ambion), anti-miR-302c (Ambion), and anti-miR-302d (Ambion) or 100 nM negative control anti-miR (Ambion) with Lipofectamine 2000 (Invitrogen) at a ratio of 1:2 for 48 h. HeLa cells or NHFs were transiently transfected with either 20 nM pre-miR-302a (Ambion) or negative control pre-miR number 1 (Ambion) with Lipofectamine 2000 according to the manufacturer's instructions for 48 h before being harvested for protein and RNA analysis; HeLa cells were transfected likewise for 24 h and NHFs for 48 h for cell cycle analysis. For luciferase experiments, HeLa cells were transfected with 10 ng pRL-CMV and 25 ng luciferase reporter vectors in addition to 40 nM of the pre-miR oligonucleotides as outlined above. For luciferase assays with promoter activity, the pGL3-miR-302 promoter construct was transfected into HeLa cells with pCAG-Myc-Oct4 and pCAG-HA-Sox2 cotransfection for 48 h.

Isolation and analysis of protein, mRNA, and miRNA. Unless otherwise indicated, protein and RNA (large and small species) were isolated from the same samples by using *mir*Vana PARIS (Ambion) as described by the manufacturer. Protein samples were resolved by 10% sodium dodecyl sulfate-polyacrylamide gel electrophoresis and transferred to a polyvinylidene difluoride membrane (GE Healthcare Bio-Sciences Corp., Piscataway, NJ). The antibodies used for immunoblotting included Oct4 (C-10; Santa Cruz), cyclin D1 (A-12; Santa Cruz), cyclin A1 (Santa Cruz), α-tubulin (DM1A; Sigma), β-actin (Sigma), Sox2 (AB5603; Chemicon International, Temecula, CA), Cdk2 (D-12; Santa Cruz), Cdk6 (H-230; Santa Cruz), and E2F1 (C-20; Santa Cruz). To synthesize cDNA, large RNA was first treated with DNase I (Invitrogen), followed by cDNA synthesis using a SuperScript first-strand synthesis system for reverse transcription-PCR (RT-PCR) (Invitrogen) as recommended by the manufacturer. Quantitative PCR (qPCR) was performed by using brilliant Sybr green qPCR reagent (Stratagene, La Jolla, CA) with the qPCR primer pairs listed in Table S1 in the supplemental material. The relative expression levels were normalized to the level of human glyceraldehyde-3-phosphate dehydrogenase (GAPDH). To analyze miRNA, a mirVana qRT-PCR miRNA detection kit (Ambion) and mirVana qRT-PCR primer sets for miR-302a, -b, -c, and -d, (Ambion) were used according to the manufacturer's directions. The relative expression levels were normalized to that of 5S (Ambion).

EMSAs. Nuclear extracts were prepared from BG-01 cells by using the method of Dignam et al. (8) with modifications as described below. The cells were harvested by being washed and scraped with phosphate-buffered saline (PBS) and resuspended on ice for 10 min in cold buffer A (10 mM HEPES, pH 7.9, 1.5 mM $MgCl_2$, 10 mM KCl, 0.5 mM dithiothreitol [DTT], protease inhibitor cocktail), followed by lysis with a Wheaton homogenizer. After centrifugation, intact nuclei resuspended in buffer B (20 mM HEPES, pH 7.9, 25% glycerol, 420 mM NaCl, 1.5 mM $MgCl_2$, 0.2 mM EDTA, 0.5 mM DTT, 1% protease inhibitor cocktail) were incubated on ice for 30 min. The nuclear extracts were then dialyzed for 2 h at 4°C (20 mM HEPES, pH 7.9, 20% glycerol, 100 mM KCl, 0.83 mM EDTA, 1.66 mM DTT, protease inhibitor cocktail) and stored at −80°C. Double-stranded DNA oligonucleotides 5′-end labeled with ^{32}P were used for electrophoretic mobility shift assays (EMSAs) (see Table S4 in the supplemental material for sequences). Ten picomoles of the WT sense strand oligonucleotide was end labeled and annealed with a threefold molar excess of the cold antisense strand in annealing buffer (10 mM Tris-HCl, pH 8.0, 50 mM NaCl, 1 mM EDTA). For DNA binding reactions, 3 μg of nuclear extract was added to a 10-μl volume of reaction mixture containing 1×10^5 cpm of ^{32}P-labeled double-stranded oligonucleotide and 1 μg of poly(dG-dC). The mixtures were incubated for 20 min at room temperature. A 50-fold excess of cold competitor was included prior to the addition of nuclear extract where specified. For supershift analysis, Oct4 (C-10; Santa Cruz)or Sox2 (AB5603; Chemicon International) antibodies or V5 tag antibody (Invitrogen) as a negative control was then added for 20 min. Samples were separated on 6% native polyacrylamide gels and analyzed by using a phosphorimager.

Chromatin immunoprecipitation analysis. Approximately 1×10^7 cells were used for the chromatin immunoprecipitation assay, which was carried out as previously described (17) with the following minor modifications. The antibodies used for chromatin immunoprecipitation included Oct4 (H-134; Santa Cruz), Sox2 (H-65; Santa Cruz), Nanog (AB21624; Abcam, Cambridge, MA), and normal rabbit immunoglobulin G (IgG) (Santa Cruz). qPCR was performed on DNA purified from the chromatin immunoprecipitates by using brilliant Sybr green qPCR reagent with the qPCR primer pairs listed in Table S1 in the supplemental material.

Dissection and RNA analysis of early mouse embryos. Embryonic day 3.5 (E3.5) CD1 blastocysts were flushed from dissected uteri into RNase-free PBS (Ambion). Similarly, E6.5, E7.5, and E8.5 CD1 embryos were dissected from uteri and decidua, and RNA was extracted as described above.

In situ hybridization. miRNA in situ hybridization was performed by following the Exiqon protocol with a minor modification (http://www.exiqon.com/SEEEMS/23.asp). Briefly, 4% paraformaldehyde-fixed CD-1 mouse embryos were rehydrated and pretreated with 10 μg/ml proteinase K for 5 min at room temperature and then refixed with 4% paraformaldehyde for 20 min at room temperature. Subsequently, prehybridization was carried out with hybridization mix (50% formamide, 5× SSC [1× SSC is 0.15 M NaCl plus 0.015 M sodium citrate], 0.1% Tween 20, 50 μg/ml heparin, 500 μg/ml tRNA) at 58°C for 1 h. The probes were labeled with digoxigenin, and hybridization was performed at 58°C overnight. In situ hybridization signals were detected by antidigoxigenin antibody conjugated with alkaline phosphatase (Roche, Basel, Switzerland), followed by color development by using BM purple substrate (Roche).

Immunohistochemistry. For immunohistochemistry, E6.5 CD1 embryos and their decidua were dissected in cold PBS and fixed in 4% paraformaldehyde overnight. The embryos and their decidua were then dehydrated, embedded in paraffin, and sectioned at 6 μm. The sections were rehydrated and endogenous peroxidase was quenched by treatment with hydrogen peroxide (3%) for 15 min at room temperature. The sections were then heated by microwaves in the presence of 0.1 M citrate buffer (pH 6.0) prior to incubation in 10% normal horse serum (Jackson Immunoresearch Laboratories, Inc., West Grove, PA) with an avidin-biotin blocking reagent (Vector Laboratories, Inc., Burlingame, CA). The slides were then incubated with the primary antibody, Oct4 (C-10; Santa Cruz) for 1 h at a dilution of 1:250. Nonimmune mouse IgG (Santa Cruz) was used in place of the primary antibody as the negative control, with equivalent conditions. The secondary antibody, biotinylated horse anti-mouse IgG (Vector Laboratories), was then applied at a dilution of 1:500 for 30 min, followed by a predilute label antibody for an additional 30 min (StriAviGen super-sensitive predilute label antibody; Biogenex Laboratories, San Ramon, CA). To develop the signal,

Dako liquid diaminobenzidine substrate-chromogen reagent (Dako Corporation, Carpinteria, CA) was added for 6 min. The slides were rinsed in tap water to halt the reaction, counterstained with modified Harris hematoxylin (Harelco, Gibbstown, NJ), dehydrated through a series of ethanol concentrations to xylene, and coverslipped with Permount (Fisher Scientific, Norcross, GA).

Identifying putative targets of miR-302a. We downloaded all human and mouse orthologous pairs from NCBI HomoloGene (http://www.ncbi.nlm.nih.gov/sites/entrez?db=homologene). A total of 14,481 orthologous pairs were identified, corresponding to 12,794 unique human genes. We extracted 3′UTR sequences as annotated in the UCSC Genome Browser. For each pair of UTR sequences, we searched for a 35-bp segment in which positions 2 to 8, numbered from the 3′ end, are perfectly complementary to the corresponding positions from the 5′ end (so-called "miRNA seed") (21) of miR-302a. In addition, we required that both the human and mouse segments share at least 75% base identity overall. Next, we extracted the eight-way multiz alignment (build hg17) for the identified human segments from the UCSC Genome Browser. Those that were perfectly conserved in the seed region and were overall highly conserved were selected for further investigation.

Luciferase assays. Transfected cells were lysed in 500 μl of passive lysis buffer (Promega, Madison, WI) and assayed with a dual luciferase assay (Promega) as directed by the manufacturer. The luciferase activities were expressed as the relative luciferase/*Renilla* activities, normalized to those of control transfections in each case.

Cell cycle analysis. Cells were harvested by trypsinization and counted such that approximately 1×10^6 cells were used for the analysis. The cells were washed in PBS and fixed in ice-cold ethanol overnight at 4°C. The cells were then washed in PBS and incubated in 1 ml staining solution (20 μg/ml propidium iodide Σ/10 U/ml RNaseA [Promega]/PBS) for 30 min at room temperature. The cells were examined by fluorescence-activated cell sorting (FACS) using a flow cytometer (FACSort; Becton, Dickinson and Company, Franklin Lakes, NJ), and the cell cycle populations were determined by using ModFit software (Verity Software House, Inc., Topsham, ME).

Identifying Oct4/Sox2 binding sites in the miR-302 promoter. We downloaded the 2-kb upstream promoter sequence of hsa-miR-302a from the UCSC Genome Browser (http://genome.ucsc.edu/). We searched the promoter sequence for putative Oct4 and Sox2 binding sites that are within 50 bp by using a method that is similar to MatInspector (33), with position weight matrices (PWMs) from the Transfac database (18) and PWMs created from the six well-characterized Oct4/Sox2 binding sites (5, 29, 32, 36, 41, 42). We also searched for putative Nanog binding sites with a PWM that approximated the sequence logo information from Mitsui et al. (26). The Statx PWM was taken from the Transfac database. For the region in the 2-kb promoter that contains putative Oct4, Sox2, Nanog, and Statx binding sites, we extracted the 17-way multiz alignment (build hg18) from the UCSC Genome Browser by using the Table Browser.

Statistical analysis. All data are expressed as group means ± standard errors of the means (SEM). Statistical comparisons were performed with a paired Student's *t* test. In all cases, statistical significance was defined as a P value of <0.05.

RESULTS

Oct4/Sox2 is bound to the miR-302 promoter. To determine whether any of the ESC-specific miRNAs are under the transcriptional control of Oct4 and Sox2, we analyzed putative orthologous promoter regions from human and mouse for Oct4 and Sox2 binding sites. Sequences upstream of the annotated stem-loop structure of the pre-miRNAs were scanned for Oct4 and Sox2 binding sites that were within 50 bp of each other, using a methodology that we developed to search for a pair of binding sites simultaneously by using two PWMs (see Materials and Methods). We identified Oct4 and Sox2 binding sites in the putative promoter region of a cluster of eight miRNAs located on human chromosome 4, miR-302, for human, mouse, and chicken orthologous regions (Fig. 1A). The binding sites were also conserved in other species, including primates, other mammals, and birds (see Fig. S1 in the supplemental material).

To validate this prediction, we used EMSA to determine whether Oct4 and Sox2 bound to the predicted regions. Double-stranded DNA oligonucleotides containing the predicted binding domains for Oct4 and Sox2 (Fig. 1A, B, and C; see Table S4 in the supplemental material) were labeled with ^{32}P and incubated with hESC nuclear extract. Using the Oct4 binding region probe, two major complexes of nuclear extract-bound probe, designated A and B, were detected (Fig. 1D). The complexes were competed away with a 50-fold molar excess of unlabeled WT and mutant 2 oligonucleotides, but not mutant 1 or double-mutant oligonucleotides, suggesting that Oct4 binds only to the first of the two predicted sites. The addition of Oct4 antibodies to the samples supershifted complex A (Fig. 1E), indicating that Oct4 was indeed bound to this site. The mobility of complex B was not affected by the addition of the Oct4 antibodies, suggesting that another factor was binding to this site. For EMSA with Sox2 binding sites, we made double-stranded DNA oligonucleotides with the putative Sox2 binding site that is closer to the Oct4 binding site (−471) (Fig. 1A and C). The incubation of this fragment with hESC nuclear extract yielded two complexes, A and B (Fig. 1F). Both of these complexes were competed away with a 50-fold molar excess of unlabeled WT, but not mutant, oligonucleotides, suggesting that sequence-specific factors are bound to this region of the promoter. The addition of Sox2 antibody to the samples supershifted complex B, indicating that Sox2 binds to this site on the promoter (Fig. 1G). The complex A band did not supershift in the presence of Sox2 antibody, indicating that another factor is bound to this region of the promoter.

Next, we analyzed the binding of Oct4 and Sox2 to these genomic loci in hESCs by chromatin immunoprecipitation assay using antibodies directed toward Oct4 and Sox2 and specific primers amplifying a region surrounding the predicted binding sites (Fig. 1H). The results of this chromatin immunoprecipitation analysis demonstrated that Oct4 and Sox2 were indeed bound to the putative promoter region of miR-302. As positive and negative controls, we also tested the binding of Oct4 and Sox2 to the *POU5F1* (Oct4) promoter and the GAPDH coding region, respectively. As expected, Oct4 and Sox2 both bound to the promoter region of *POU5F1* (5), but not to the GAPDH coding region. Further examination of the miR-302 promoter sequence indicated that there were also conserved Nanog binding sites downstream of the Oct4 and Sox2 binding sites (Fig. 1A). The results of a chromatin immunoprecipitation assay using Nanog-specific antibodies confirmed that Nanog also bound to the putative promoter region of miR-302 (Fig. 1H). The results of a genomic-based chromatin immunoprecipitation assay also recently identified low-resolution Oct4 and Nanog binding sites upstream of the miR-302 cluster in mESCs (24).

The miR-302 primary miRNAs are expressed as a single polycistronic transcript in two hESC lines, SNU-hES3 and Miz-hES1 (39). To determine whether the miR-302 primary miRNAs are also expressed in H1 and BG-01 hESC lines, qRT-PCR analysis was performed, using specific primers to amplify the miR-302 polycistronic transcript and mature miR-302a (Fig. 2A; see Fig. S2a in the supplemental material). The cells were cultured with RA to monitor the expression of miR-302 as they differentiated. The miR-302 polycistronic transcript was expressed in pluripotent hESC lines, but not in hESCs that had been differentiated with RA (Fig. 2A; see Fig. S2a in the

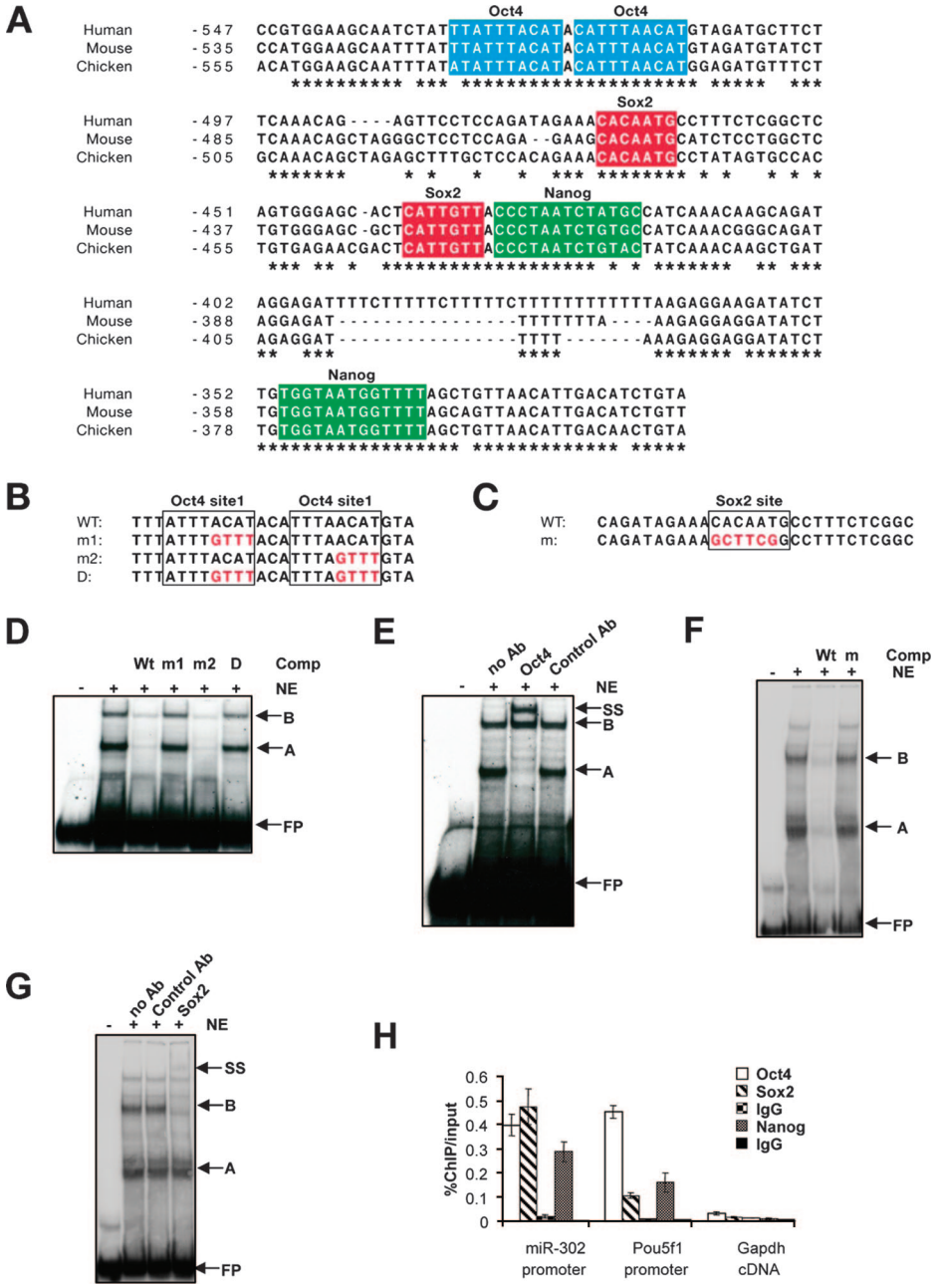

FIG. 1. Oct4, Sox2, and Nanog bind to the promoter region of the miR-302 cluster of miRNAs in hESCs. (A) Alignment of the homologous promoter regions of the miR-302 cluster of miRNAs from human, mouse, and chicken. Predicted Oct4, Sox2, and Nanog, binding sites are highlighted in blue, red, and green, respectively. Asterisks indicate sequence homology. (B) Sequences of the double-stranded DNA probe containing the predicted WT Oct4 binding domain and the mutant 1, mutant 2, and double-mutant oligonucleotides (m1, m2, and D) used in EMSA analysis. (C) Sequence of the double-stranded DNA probe containing the predicted Sox2 binding site that is closer to the Oct4 binding sites (−471). m, mutant. (D and E) EMSA analysis performed with extracts of BG-01 cells with the Oct4 binding site. (D) EMSA with 50-fold cold competitors of WT, mutant 1, mutant 2, and double-mutant (m1, m2, and D) oligonucleotides. (E) Supershift with Oct4 antibody. (F and G) EMSA analysis performed with the Sox2 binding site. (H) Oct4, Sox2, and Nanog bind to the promoter region of miR-302 in pluripotent cells. hESCs were cross-linked with formaldehyde, and chromatin was prepared by sheering DNA by sonication. The fragmented chromatin was then immunoprecipitated with antibodies directed toward Oct4, Sox2, Nanog, and nonspecific antibodies (IgG). DNA associated with each of the chromatin immunoprecipitates was amplified by qRT-PCR with primers specific for the promoter regions of miR-302 and Oct4 or GAPDH cDNA as a negative control. The qRT-PCR results shown here are representative examples of the results of at least three experiments performed with the BG-01 cell line. Error bars represent standard deviations. The two major complexes of nuclear extract-bound probe, designated A and B, are indicated with arrows to the right of the gels. +, present; −, absent; FP, free probe; SS, supershift; Comp, competitor; NE, nuclear extract; Ab, antibody; ChIP, chromatin immunoprecipitation.

supplemental material). Similarly, undifferentiated cells also expressed miR-302a very abundantly. As a control, Oct4 mRNA expression was also analyzed and was only detected in undifferentiated pluripotent cells (Fig. 2A; see Fig. S2a in the supplemental material). Decreased Oct4 protein expression (Fig. 2B; see Fig. S2b in the supplemental material) paralleled the relative decreases in miR-302 and miR-302a expression throughout the differentiation period, consistent with Oct4

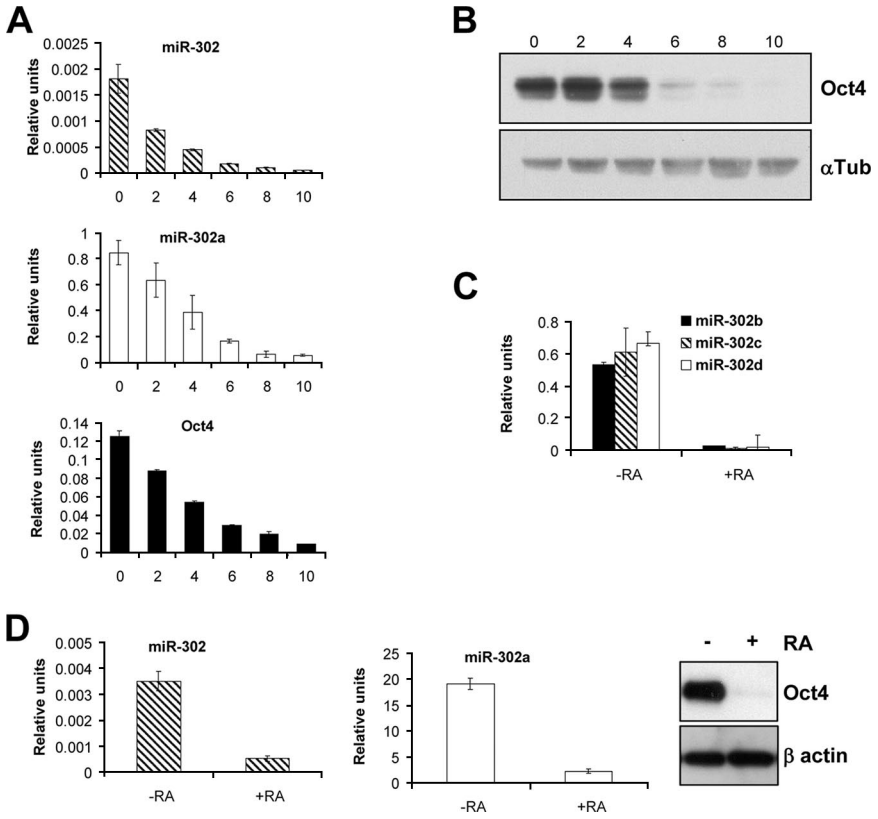

FIG. 2. Oct4 expression correlates with expression of miR-302 miRNAs during RA treatment. (A, B, and C) hESCs exposed to 1 μM RA for 0 to 10 days were harvested, and RNA and protein extracted from whole-cell lysates were analyzed by qRT-PCR with primers specific to miR-302 transcript, miR-302a, and Oct4 (A); by Western blotting with antibodies specific to Oct4 and α-tubulin (Tub) (B); and by qRT-PCR with primers specific to miR-302b, -c, and -d (C). (D) NTERA2 cells exposed to RA for 10 days were analyzed as described for panel A with primers specific to the miR-302 transcript and miR-302a or by Western blotting with antibodies specific to Oct4 and β-actin. The qRT-PCR and Western blots shown here are representative examples of the results of three experiments performed with H1 cells or NTERA2 cells. +, treated with RA; −, not treated with RA. Error bars represent standard deviations.

functioning as a transcriptional activator, rather than repressor, of this gene cluster. We also tested the expression of three other mature miRNAs from this cluster, miR-302b, -c, and -d, in hESCs (Fig. 2C; see Fig. S2c in the supplemental material) and showed that these miRNAs are highly expressed in undifferentiated cells relative to their levels of expression in differentiated cells. The miR-302 polycistronic transcript and miR-302a were similarly expressed in Oct4-positive embryonal carcinoma NTERA2 cells, but not in NTERA2 cells treated with RA (Fig. 2D). Intriguingly, the levels of mature miR-302a, -b, -c, and -d seem to be extremely high in undifferentiated cells, roughly equivalent to the level of 5S rRNA in hESCs.

Oct4/Sox2 is required for miR-302a expression. To determine whether Oct4 and Sox2 transcription factors directly activate the miR-302 promoter, we cloned a 1-kb fragment of the miR-302 promoter (~1 kb upstream of the predicted transcription start site) into the pGL3 vector (Fig. 3B). We introduced this construct into hESCs that had been depleted of Oct4 and Sox2 proteins by using siRNAs (Fig. 3A). When the pGL3-miR-302 construct was introduced under conditions of Oct4 and Sox2 depletion, we observed an ~65% reduction in luciferase activity compared to the luciferase activity with control siRNA (Fig. 3B). These results suggest that the miR-302 gene is under the direct control of Oct4 and Sox2 transcription factors in hESCs.

To further validate that Oct4 and Sox2 are required for miR-302 expression, we analyzed the expression of miR-302a in hESCs transfected under conditions of Oct4 and Sox2 knockdown. The expression level of miR-302a under Oct4/Sox2-depleted conditions was reduced by more than 50% in comparison with the level in cells transfected with nontargeting siRNAs (Fig. 3C and D). Oct4 knockdown alone leads to a small decrease in miR-302a levels, whereas Sox2 knockdown alone has a minimal effect. These data show that the expression of miR-302a is dependent on Oct4/Sox2 in hESCs and suggest that Oct4 and Sox2 function as transcriptional activators.

We also introduced pGL3-miR-302 into HeLa cells under conditions of overexpression of Oct4 and Sox2 (Fig. 3E). We observed about a 1.6-fold increase in luciferase activity in the presence of Oct4 and Sox2 transcription factor in HeLa cells (Fig. 3F).

miR-302 is expressed in early embryogenesis. We next analyzed the expression of the miR-302 transcript and miR-302a in early mouse embryos to determine whether the miR-302 miRNAs are expressed at the same developmental time points and in the same tissues as Oct4. qRT-PCR analysis was per-

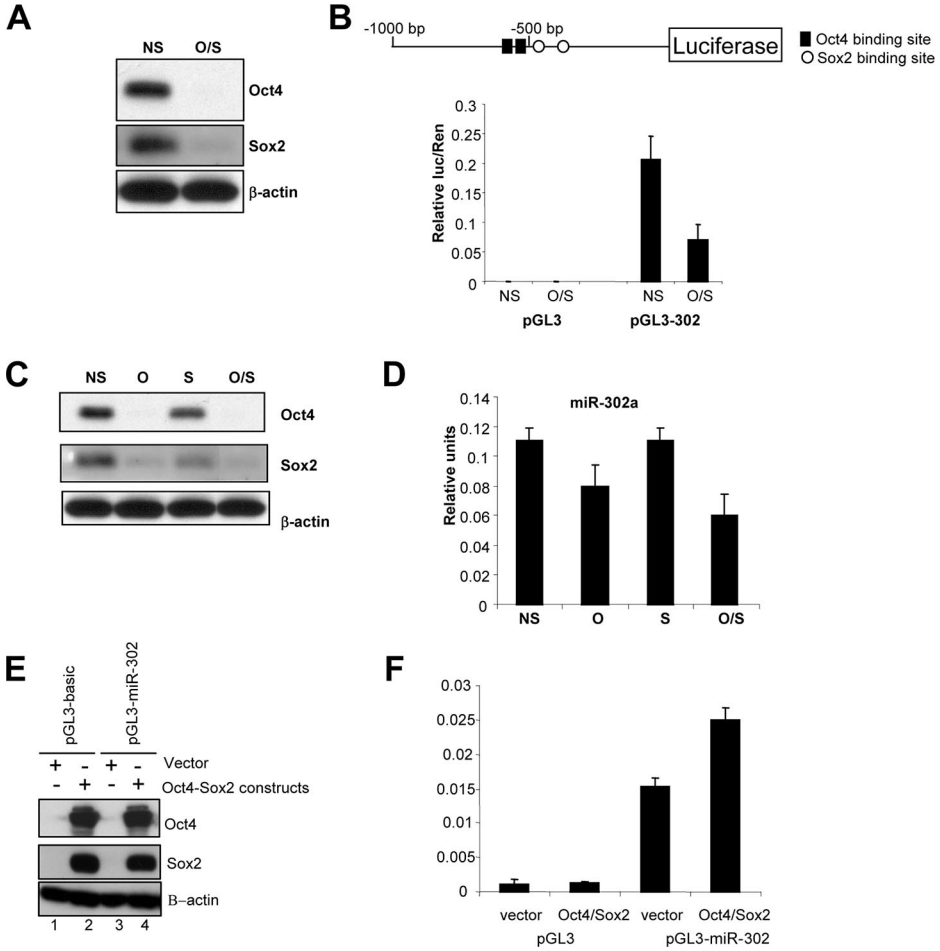

FIG. 3. Oct4 and Sox2 transcription factors are required for expression of miR-302 miRNAs. (A) BG-01 cells were transfected with 200 nM nonspecific control (NS) or 100 nM each of Oct4 and Sox2 (O/S) siRNA oligonucleotides as described in Materials and Methods, and whole-cell extracts were made. Oct4, Sox2, and β-actin protein expression levels were analyzed by Western blotting with specific antibodies. (B) BG-01 cells were transfected with pGL3-Basic or pGL3-miR-302 with either nonspecific control siRNA (NS) or Oct4/Sox2 siRNA (O/S) as described for panel A for 48 h. In addition, all samples were transfected with pRL-CMV as a transfection control. Cell extracts were then harvested and analyzed for relative luciferase activity. A schematic of the cloned promoter region in pGL3-miR-302 is shown. luc/ren, luciferase/*Renilla* activities. (C) BG-01 cells were transfected with 100 nM of nonspecific control (NS), Oct4 siRNA (O), Sox2 siRNA (S), or Oct4/Sox2 siRNA (O/S) as described for panel A, and Oct4, Sox2, and β-actin protein expression levels were analyzed by Western blotting with specific antibodies. (D) qRT-PCR was used to analyze the relative expression levels, normalized to 5S rRNA levels, of the mature miR-302a miRNA in the siRNA-depleted cells. (E) HeLa cells were transfected with pGL3-Basic or pGL3-miR-302 with pCAG-Myc-Oct4 and pCAG-HA-Sox2 cotransfection or empty vector cotransfection. Western blots were probed with Oct4, Sox2, and β-actin antibodies. +, present; −, absent. (F) HeLa cell lysates were analyzed for relative luciferase activities; data are expressed in relative units.

formed on RNA isolated from mouse embryos at developmental stages E3.5, E6.5, E7.5, and E8.5 (Fig. 4A). The miR-302 polycistronic transcript was expressed at E6.5, E7.5, and E8.5, again corresponding well with the relative levels of Oct4 at these stages. miR-302a was also expressed at these developmental time points. While the expression of the miR-302 transcript peaked at E6.5, the expression of miR-302a was greatest at E7.5, suggesting that the processing of the mature miRNA may lag behind the expression of the primary transcript. Despite robust expression of Oct4 at E3.5, however, there was very little expression of either the miR-302 polycistronic transcript or miR-302a at this stage.

To determine the tissue-specific expression of miR-302a during embryogenesis, we performed in situ hybridization with E6.5 and E7.5 embryos. The complementary sequence of miR-302a, linked to digoxigenin, was used as a probe, and a scrambled probe was used as the negative control. At E6.5, the expression of miR-302a is largely confined to the epiblast (Fig. 4B), a region that is also known to be Oct4 positive, as confirmed by the results of immunohistochemistry (see Fig. S3 in the supplemental material). At E7.5, miR-302a is also expressed in the same region as Oct4 (11). The results of these experiments confirm that miR-302 is expressed at the same developmental time points during embryogenesis as Oct4.

miR-302 miRNAs target cell cycle regulators and promote an ESC-like cell cycle. We predicted potential targets of mature miR-302 miRNAs based on the fact that four of the eight mature miRNAs (miR-302a, -b, -c, and -d) were highly homologous, particularly in the 5′ seed region (39) to which miRNAs bind and which is complementary to the corresponding posi-

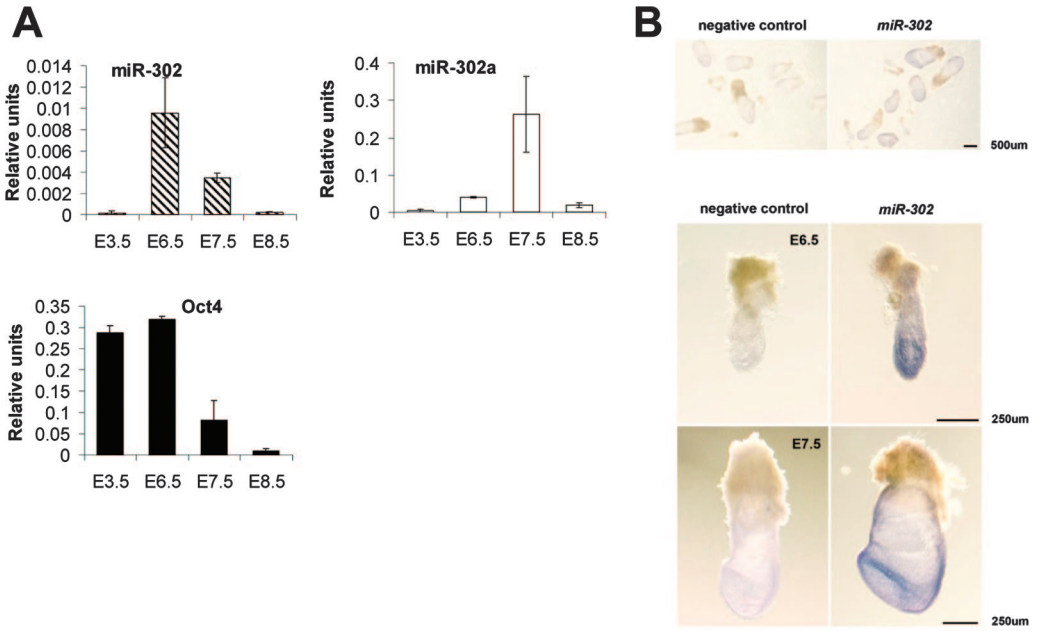

FIG. 4. miR-302 is expressed in early embryogenesis. (A) CD1 embryos were isolated at E3.5, E6.5, E7.5, and E8.5 points of development. RNA was extracted and analyzed by qRT-PCR for levels of Oct4 mRNA, miR-302 transcript, and miR-302a, and the average relative expression levels are shown. (B) E6.5 and E7.5 embryos were analyzed by in situ hybridization with probes for miR-302a (miR-302) and a negative control, as indicated. Top, E6.5 and E7.5 embryos in the same field; bottom, E6.5 and E7.5 embryos, as indicated. Bars show sizes as indicated.

tions in the 3′UTR of target mRNAs (1). This suggested that these miRNAs were targeting the same mRNAs. As described in Materials and Methods, we generated a list of potential targets subject to posttranscriptional repression by miR-302a, -b, -c, and -d (see Fig. S4 in the supplemental material). We noticed immediately that many of these targets were cell cycle regulators.

In differentiated cells, G_1 phase is generally the longest phase of the cell cycle, and in ESCs, G_1 phase is very short (approximately 1 to 2 h). Retinoblastoma protein (Rb) is maintained in a hyperphosphorylated state throughout G_1 in ESCs (37). We hypothesized that ESCs may express a negative regulator of G_1 phase, such as miR-302, that is not present in differentiated cells. By using FACS analysis to evaluate the cell cycle profiles of propidium iodide-stained hESCs progressively undergoing RA-induced differentiation, we began to investigate the effect of miR-302 expression on cell cycle progression (see Fig. S5a in the supplemental material). In pluripotent hESCs, the majority (approximately 50%) of cells were in S phase, consistent with observations reported by other groups (10, 37). As cells progressively differentiated, the cell cycle profiles shifted from a high S-phase population to a high G_1-phase population, while there was little change in the number of cells in G_2/M. Additionally, in samples differentiated with RA for 10 days, there were approximately one-half the number of cells compared to the number of pluripotent cells (see Fig. S5b in the supplemental material), suggesting that the cell cycle time had slowed down. Taken together, our observations raise the possibility that as hESCs differentiate, cell cycle populations progressively shift from a short G_1-phase cell cycle to a long G_1-phase cell cycle and that this shift is mediated by miR-302 attenuation of cell cycle regulator expression in pluripotent cells. We also observed the same increase in the population of G_1-phase NTERA2 cells that had been differentiated with RA (see Fig. S5c in the supplemental material). To test this, we decided to investigate the effect of expressing miR-302a in nonpluripotent cells.

We transfected HeLa cells with pre-miR-302a or a negative control pre-miR. The results of cell cycle analysis demonstrated that the expression of miR-302a caused increases in the populations of S-phase ($P < 0.01$) (Fig. 5A and B) and G_2/M-phase ($P < 0.05$) cells. Additionally, we observed a decrease in the number of cells in G_1 phase ($P < 0.01$). Similar results were observed when the experiment was repeated with MCF-7 cells (see Fig. S6 in the supplemental material). Due to the fact that both of these cell lines are transformed, we also repeated the experiment with a primary cell line, NHFs. When NHFs were transfected with pre-miR-302a, their cell cycle profile shifted to an increased S-phase population ($P < 0.01$) (Fig. 5C and D) and a decreased G_1-phase population ($P < 0.05$). Since the exogenous expression of miR-302 promoted cell cycle profiles reminiscent of a more-ESC-like cell cycle distribution (10, 38), we next decided to test the function of miR-302a in the cell cycle of pluripotent cells.

To investigate the effect of miR-302 expression on the hESC cell cycle, we inhibited the function of miR-302a, -b, -c, and -d in hESCs with single-stranded sequence-specific nucleic acid inhibitors (anti-miR-302). In hESCs transfected with anti-miR-302, mature miR-302a levels were decreased due to the fact that the anti-miR inhibitors bind irreversibly to the miRNAs, causing them to be unavailable both functionally and for the analysis (see Fig. 7A.). Cell cycle analysis of hESCs transfected with anti-miR-302 showed an increase in the population of G_1-phase cells compared to this population in cells transfected

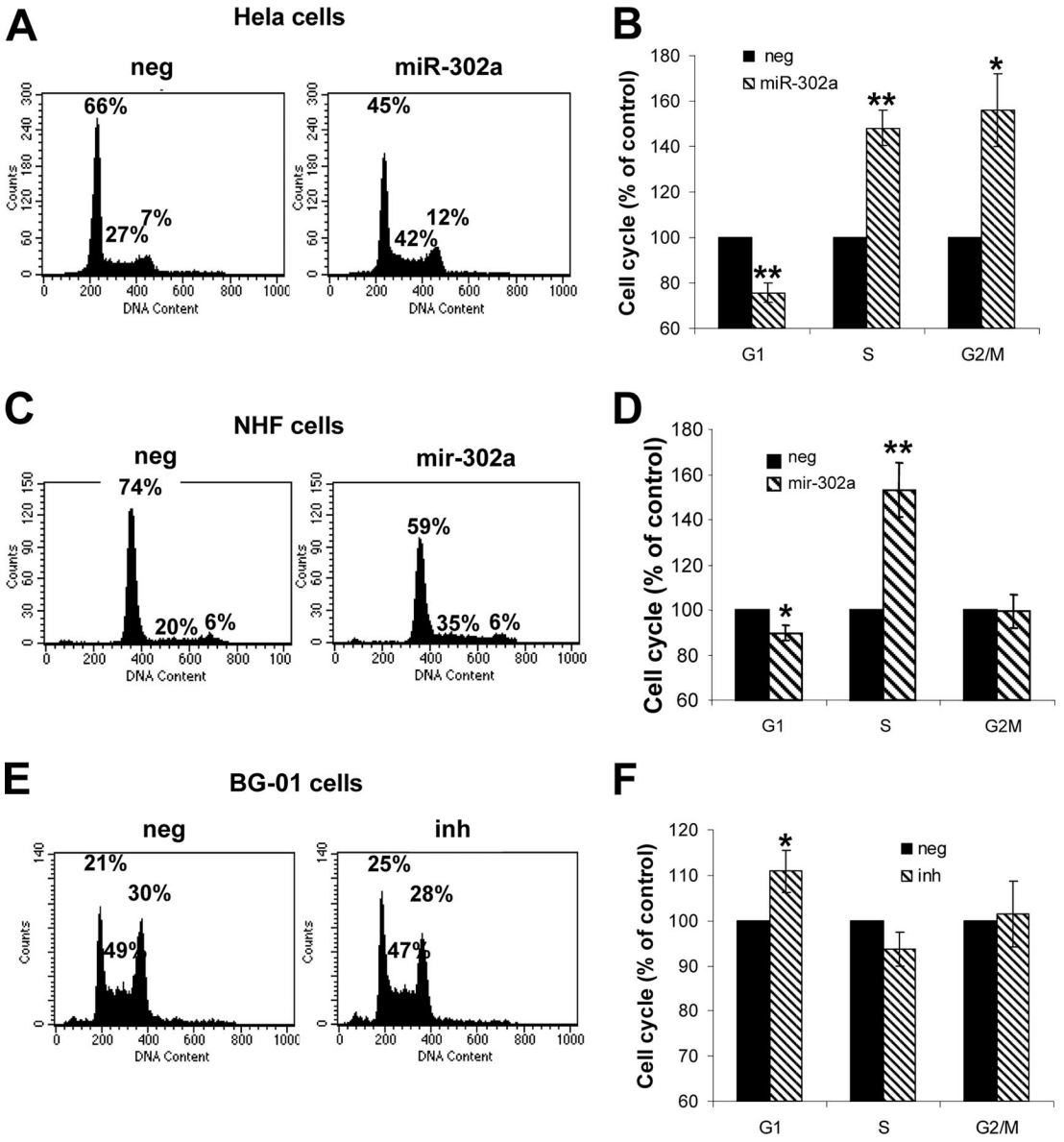

FIG. 5. The expression of miR-302 cluster miRNAs is associated with a short G_1 phase. HeLa cells were transfected with pre-miR-302a or negative (neg) control pre-miR. Cell cycle analysis was performed by FACS. Percentages of cells in G_1, S, and G_2/M are depicted in the graph. Shown here are a typical FACs analysis plot (A) and a graph representing the means ± SEM of the results of three independent experiments (B). (C and D) NHFs were transfected with pre-miR-302a or negative control pre-miR. Shown here are a typical FACs analysis plot (C) and a graph representing the means ± SEM of the results of four independent experiments (D). (E and F) BG-01 cells grown on Matrigel plates were transfected by nucleofection with 200 pmol each miR-302a, -b, -c, and -d inhibitors (inh) or the negative control, as described in Materials and Methods, and cell cycle analysis was performed by FACS. Percentages of cells in G_1, S, and G_2/M are depicted in the graph. Shown here are a typical FACs analysis plot (E) and a graph representing the means ± SEM of the results of three independent experiments (F).

with the control, a random-sequence nucleic acid inhibitor ($P = 0.05$) (Fig. 5E and F). This result demonstrated that the inhibition of miR-302 in hESCs causes a change in the cell cycle profile, specifically by increasing the population of cells in G_1 phase, a trend consistent with a differentiated cell type.

miR-302 miRNAs posttranscriptionally repress cyclin D1 expression in hESCs. Of the candidate miR-302 targets, cyclin D1 was an intriguing possibility because ESCs are known to have low levels of cyclin D1 expression (38) and a short G_1 phase that is regulated by pathways other than the cyclin D/Cdk4-mediated regulation of Rb (37). Moreover, the predicted miR-302a binding domain in the cyclin D1 3′UTR is highly conserved (see Fig. S7 in the supplemental material). To determine if cyclin D1 is indeed a target of posttranscriptional regulation by miR-302a, -b, -c, and -d, we first examined the expression of cyclin D1 in hESCs that had been differentiated with RA. The results of the analysis of hESC lysates by Western blotting and qRT-PCR demonstrated that as differentiation proceeded, cyclin D1 protein levels increased, but there was little change in cyclin D1 mRNA levels (Fig. 6A; see Fig.

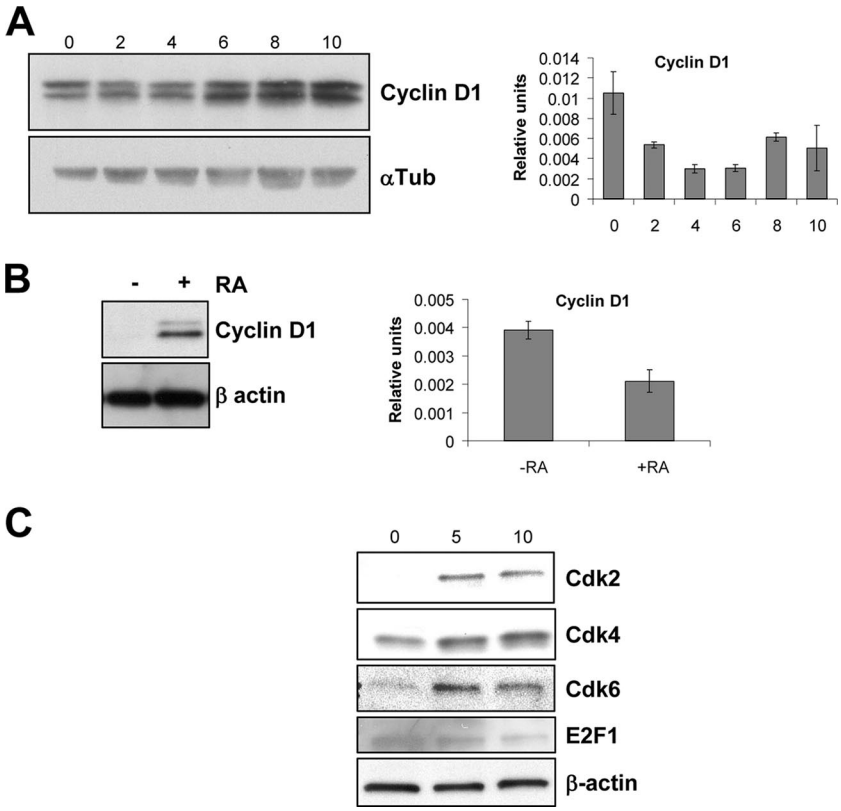

FIG. 6. Expression analysis of the potential miR-302 target cyclin D1. (A) Western blot analysis of cyclin D1 protein expression and qRT-PCR analysis of cyclin D1 mRNA in extracts of H1 cells treated with RA as described in the Fig. 2 legend. αTub, α-tubulin. (B) Western blot and qRT-PCR analysis of cyclin D1 expression in NTERA2 cells. +, treated with RA; −, not treated with RA. (C) Western blot analysis of Cdk2, Cdk4, Cdk6, and E2F1 protein expression in extracts of H1 cells treated with RA.

S8a in the supplemental material). We also observed the same results in NTERA2 cells differentiated with RA (Fig. 6B). The change in cyclin D1 expression levels cannot be attributed to any contribution from the MEF coculture cells, as these cells alone do not demonstrate any change in cyclin D1 expression in the results of a similar experiment (see Fig. S8b in the supplemental material). These data are consistent with cyclin D1 protein and mRNA expression patterns in differentiating mESCs (16) and with cyclin D1 being a target of miR-302 translational repression.

We also screened other putative targets of miR-302 which are known to be involved in cell cycle regulation, such as E2F1, Cdk2, and Cdk6 (Fig. 6C). We also screened the cyclin D1 binding partner, Cdk4, as cyclin D1/Cdk4 complexes display low levels of kinase activity in mESCs. The results of sequence analysis revealed a potential miR-302a binding site just upstream of the Cdk4 3′UTR (see Fig. S7d in the supplemental material). Although this site is located in the coding region, miRNAs are predicted to bind to open reading frames of human targets (20, 25) and have been shown to bind to coding regions of plant mRNAs (23). Kinases Cdk2, Cdk4, and Cdk6 are all expressed at low levels in the pluripotent cells and at increased levels in cells differentiated by treatment with RA. Therefore, miR-302 may target these mRNAs to regulate their expression. The potential target E2F1 demonstrated no change in its expression level over the course of differentiation.

To determine if in fact miR-302 was posttranscriptionally repressing cyclin D1 in hESCs, we inhibited the function of miR-302a, -b, -c, and -d with single-stranded sequence-specific nucleic acid inhibitors (anti-miR-302). In hESCs transfected with anti-miR-302, mature miR-302a levels were decreased due to the fact that the anti-miR inhibitors bind irreversibly to the miRNA, causing them to be unavailable both functionally and for the analysis (Fig. 7A). Under these conditions, the cyclin D1 protein level was increased, but there was no change in the cyclin D1 mRNA level. This suggested that miR-302 translationally represses cyclin D1 expression in hESCs. Notably, the Oct4 and Sox2 protein levels were equivalent in cells transfected with anti-miR-302 and the control, suggesting that these cells have not differentiated.

We predicted from the results of these experiments that if miR-302 was acting as a negative regulator of cyclin D1 protein levels in hESCs, the introduction of miR-302a into differentiated cells would lead to a decrease in cyclin D1 protein levels. We tested this directly by transfecting HeLa cells with pre-miR-302a, a precursor molecule of the mature miRNA, or with negative control pre-miR, a random-sequence precursor molecule that does not code for any known miRNA. The results of the qRT-PCR analysis of cell extracts demonstrated that miR-302a was generated in cells transfected with pre-miR-302a, but not in cells transfected with the negative control pre-miR (Fig. 7B). Additionally, the levels of an endogenous miRNA, miR-

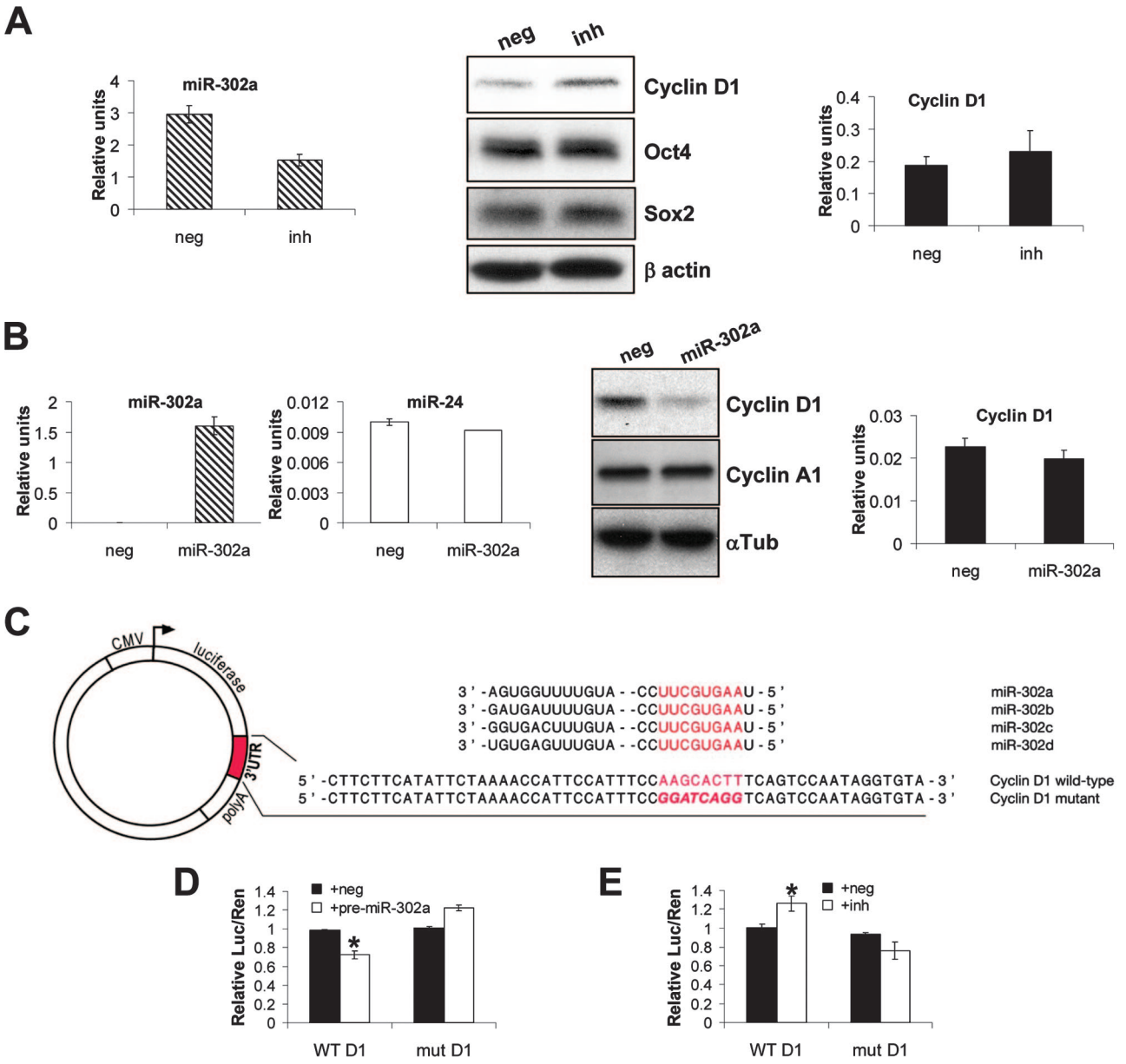

FIG. 7. miR-302a binds to the 3′UTR of cyclin D1 to posttranscriptionally repress protein expression. (A) BG-01 cells grown on Matrigel plates were transfected by nucleofection with 200 pmol each of miR-302a, -b, -c, and -d inhibitors (inh) or the negative control (neg), as described in Materials and Methods, and protein and RNA were isolated from whole-cell extracts. qRT-PCR analysis of mature miR-302a levels upon transfection with anti-miR-302 inhibitors was performed. Cyclin D1 and β-actin protein expression levels were analyzed by Western blotting with specific antibodies. RNA isolated from the same cell lysates was analyzed by qRT-PCR with primers specific for cyclin D1 mRNA, and the results were plotted as relative units. (B) Twenty nanomolar pre-miR-302a or negative control pre-miR (neg) was transfected into HeLa cells in duplicate, as indicated. Results of qRT-PCR analysis of mature miR-302a levels upon transfection are shown. The endogenous miRNA miR-24 was also analyzed by qRT-PCR. Protein isolated from whole-cell extracts was analyzed by Western blotting with antibodies directed toward cyclin D1 or α-tubulin (αTub). RNA isolated from the same cell lysates was analyzed by qRT-PCR with primers specific for cyclin D1 mRNA, and the results were plotted as relative units. (C) Schematic of miR-302a, -b, -c, and -d binding site in cyclin D1 3′UTR inserted into the pMIR-REPORT luciferase reporter vector. A section of the cyclin D1 3′UTR containing the predicted miR-302a, -b, -c, and -d binding site (highlighted in red) was inserted downstream of luciferase in the pMIR-REPORT vector. Predicted pairing regions within the WT cyclin D1 3′UTR are noted in red, while those residues altered in the cyclin D1 mutant construct are bolded and italicized. (D) HeLa cells were transfected with the WT cyclin D1 or mutant cyclin D1 vectors, as indicated, with either pre-miR-302a or negative control pre-miR (neg). Additionally, all samples were transfected with pRL-CMV. Cell extracts were then harvested and analyzed for relative luciferase activities. Shown here are the means ± SEM of the results of three independent experiments. (E) BG-01 cells were transfected with the luciferase vectors as described for panel D. Additionally, 25 nM each of miR-302a, -b, -c, and -d inhibitor (inh) or 100 nM anti-miR negative control (neg) was added, as described in Materials and Methods. Relative luciferase activities were then analyzed. Shown here are the means ± SEM of the results of three independent experiments. An asterisk indicates a P value of <0.05. Luc/Ren, luciferase/*Renilla* activities; D1, cyclin D1; mut, mutant.

24, were unaffected by transfection with pre-miR-302a. Cyclin D1 protein was significantly diminished in cells transfected with pre-miR-302a compared to its level in cells transfected with the negative control pre-miR, while cyclin D1 mRNA was expressed at the same level in cells transfected with pre-miR-302a and negative control pre-miR. Additionally, the level of cyclin A1 protein, which is not a potential target of miR-302a, was unaffected by transfection with pre-miR-302a.

To resolve whether miR-302a regulates cyclin D1 directly or indirectly, we inserted the region of the cyclin D1 3′UTR predicted to bind to miR-302a into the 3′UTR of a luciferase reporter plasmid (Fig. 7C). We also generated a negative control reporter plasmid in which the cyclin D1 3′UTR was mutated by changing the nucleotides within the 8-bp site of complementarity to the 5′ seed regions of the miRNAs. HeLa cells were transfected with one of these plasmids in the presence of either pre-miR-302a or negative control pre-miR (Fig. 7D). There was a decreased level of relative luciferase activity in cells expressing miR-302a compared to the level in the negative control after transfection with the WT cyclin D1 UTR plasmid ($P < 0.05$), whereas the cells transfected with the mutant cyclin D1 UTR plasmid did not have a decrease in relative luciferase activity, suggesting that miR-302a directly regulates the expression of cyclin D1. As miR-302a is not endogenously expressed in these cells, we wanted to verify this result using pluripotent cells that express mature miR-302 miRNAs. In this case, we transfected hESCs with the vectors described above in the presence of either specific inhibitors of miR-302a, -b, -c, and -d (anti-miR-302) or a negative control inhibitor (anti-miR negative control) (Fig. 7E). In cells transfected with the WT cyclin D1 UTR plasmid, the inhibition of miR-302a, -b, -c, and -d caused an increase in relative luciferase activity compared to the luciferase activity in the anti-miR negative control cells ($P < 0.05$), whereas no such increase was observed in cells transfected with the cyclin D1 mutant UTR plasmid. These data strongly suggest that miR-302a, -b, -c, and -d translationally repress cyclin D1 in hESCs.

The Cdk4 protein levels were increased in response to the inhibition of miR-302 in hESCs (Fig. 8A), suggesting that Cdk4 is also a target of miR-302. Additionally, the transfection of pre-miR-302a into HeLa cells caused the Cdk4 protein levels to decrease (Fig. 8B), demonstrating that Cdk4 is a target of miR-302 even in a heterologous system.

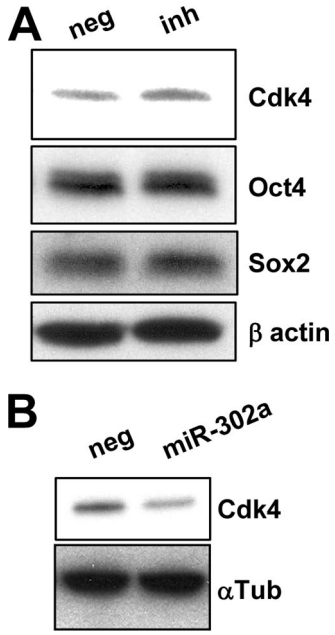

FIG. 8. Expression analysis of the potential miR-302 target Cdk4. (A) Western blot analysis of Cdk4 protein expression in BG-01 cells transfected with negative control (neg) or miR-302a, -b, -c, and -d inhibitors (inh) as described for Fig. 7A. (B) Western blot analysis of Cdk4 protein expression in HeLa cells transfected with negative control (neg) or pre-miR-302a as described for Fig. 7B. αTub, α-tubulin.

DISCUSSION

It is clear from the results of recent analyses using human and mouse systems that the homeodomain proteins Oct4, Sox2, and Nanog are at the top of a transcriptional hierarchy that is responsible for the initiation and/or maintenance of the expression of a group of genes that positively regulate the pluripotent phenotype and repress those genes associated with differentiation (2, 24). The results of recent studies have also implicated transcription factors associated with cell cycle control, including Myc and Klf4, in reprogramming differentiated cells to pluripotent cells (40). Less well understood are the mechanisms by which these individual genes participate in the multiple downstream signaling pathways and regulatory cascades. The findings reported here may suggest a connection between the transcriptional activation of the miR-302 cluster by Oct4 and Sox2 and the translational repression of cell cycle regulators, including cyclin D1, in hESCs.

The expression of tissue-specific miRNAs is regulated by transcription factors controlling gene expression networks associated with cell-type specificity (6, 9, 34). We have shown that miR-302 is expressed in the same cells as Oct4 (Fig. 2; see Fig. S2 in the supplemental material). We also show that Oct4 and miR-302 are expressed concomitantly and in the same tissues during early stages of mouse development (Fig. 4; see Fig. S3 in the supplemental material), and it is likely that this gene cluster plays an important role in pluripotent cells in vivo.

Oct4, Sox2, and Nanog all bind to the putative promoter region of the miR-302 cluster of miRNAs (Fig. 1D to H), and Oct4 and Sox2 are required for the expression and transcriptional activation of miR-302 in hESCs (Fig. 3), suggesting that these factors are transcriptionally activating the miR-302 primary transcript in pluripotent cells. As is the case for other genes regulated by Oct4 and Sox2, the binding sites for these factors are located in close proximity to one another, consistent with the idea that Oct4 and Sox2 bind their targets synergistically (35). The predicted binding sites for these factors are well conserved upstream of similar polycistronic clusters of miR-302 homologs among vertebrates that develop as amniotic embryos (Fig. 1A; see Fig. S1 in the supplemental material), suggesting that the expression of this gene by Oct4 and Sox2 is important for conserved mechanisms during development. Interestingly, the zebrafish genome contains many copies of a related cluster of miRNAs, miR-430a-b-c (12). Like the miR-302 cluster, this cluster of miRNAs is expressed at early embryonic stages and is additionally required for brain morphogenesis (12, 13), thus sharing a similar phenotype with the

zebrafish *POU5F1* ortholog, *spg* (3). Taken together, these data suggest that Oct4 and miR-302 family members are part of an ancestrally conserved mechanism.

We have shown that one function of four of the mature miRNAs from the miR-302 cluster, miR-302a, -b, -c, and -d, is to repress the posttranscriptional expression of cyclin D1 (Fig. 7). Collectively, the inhibition of these miRNAs causes upregulation of cyclin D1 protein in hESCs (Fig. 7A), although this likely requires only a single miRNA for each individual transcript, due to the functional redundancy of the homologous 5′ seed region of the miRNAs. Importantly, the expression of cyclin D1 in hESCs is not completely abolished by the miRNAs in pluripotent cells; instead, these factors have a dampening effect on the protein's translation.

The exogenous expression of miR-302a in primary and transformed cells increased the number of S-phase cells and decreased the number of G_1-phase cells (Fig. 5). This phenotype is reminiscent of the unique cell cycle characteristics of mESCs and epiblast cells (10, 37). More significantly, the inhibition of miR-302a, -b, -c, and -d in hESCs caused an increase in the number of cells in G_1 phase, suggesting that miR-302 is a negative regulator of G_1 and/or promotes entry into S phase. The control of rapid advancement through G_1 has been proposed to be fundamental to stem cell identity in vivo (14), although specific factors have yet to be identified. Additionally, in the absence of functional miRNAs, mESCs are only able to grow when they demonstrate an augmented G_1 population (27), suggesting that Dicer mutants fail to generate factors that cause rapid progression through G_1 phase. Moreover, the results of studies of *Drosophila melanogaster* demonstrate that miRNAs are required to bypass the G_1 checkpoint in germ line stem cells (14), suggesting that an extended G_1 phase may be detrimental to stem cell identity.

While we have focused on cyclin D1 as a target of miR-302 translational repression, it is unlikely that the change in the cell cycle distribution caused by the expression of miR-302 in transformed and primary cells is uniquely dependent on this cyclin alone. In fact, miRNAs are thought to typically affect hundreds of targets, and this is likely also the case for miR-302. We demonstrate here that miR-302 is in fact also targeting Cdk4 (Fig. 8). We have also identified a number of potential miR-302 targets which are cell cycle regulators (see Fig. S4 in the supplemental material), and many of these, such as Rb, E2F1, p130, Cdk2, and Cdk6, are intricately involved in the regulation of G_1 phase (see Fig. S4 in the supplemental material). Further testing of these individual targets will validate their roles in miR-302-mediated cell cycle regulation in ESCs. Therefore, the miR-302-mediated regulation of cell cycle progression may be attributable to its targeting multiple mRNAs. In fact, Linsley et al. found that transfection with an unrelated miRNA, miR-16, caused an accumulation of cells in G_1 (22). However, Linsley et al. found that to mimic the effect of miR-16 inhibition on cell cycle progression, the expression of four target genes had to be repressed by siRNA before a similar cell cycle effect was observed (22), suggesting that miR-16 coordinately regulates multiple targets which collectively cause the observed G_1 accumulation. This suggests that miR-302 may also be coordinately targeting multiple G_1-phase regulators in addition to cyclin D1 and Cdk4 to act as a negative regulator of G_1.

Our data suggest that Oct4/Sox2 is transcriptionally activating and required for the expression of miR-302. In hESCs, miR-302 translationally represses cyclin D1, which may link Oct4/Sox2 to the cell cycle regulation of pluripotent cells. Indeed, the expression of miR-302 promotes an ESC-like cell cycle profile, while the inhibition of miR-302 in hESCs causes a shift in the cell cycle to resemble a more-differentiated population. Since the therapeutic potential of hESCs depends on their unique ability to maintain pluripotency and self-renew in vitro, understanding the factors that mediate these processes, such as the transcriptional control of cell cycle regulation, is critical to realizing the potential of hESCs in disease therapies.

ACKNOWLEDGMENTS

We thank Lois Annab for maintenance of MEFs; Paul Wade, Sayura Aoyagi, and Jeff Card for helpful discussion; Gina Goulding and Trisha Castriano for assistance with mouse embryology; Ajeet Singh for mouse embryonic samples; Julie Foley for assistance with immunohistochemistry; Grace Kissling for assistance with statistical analysis; and Carl Bortner and Maria Sifre for assistance with flow cytometry.

This research was supported by the Intramural Research Program of the National Institute of Environmental Health Sciences, NIH, project number Z01 ES071006-09.

REFERENCES

1. **Bartel, D. P.** 2004. MicroRNAs: genomics, biogenesis, mechanism, and function. Cell **116:**281–297.
2. **Boyer, L. A., T. I. Lee, M. F. Cole, S. E. Johnstone, S. S. Levine, J. P. Zucker, M. G. Guenther, R. M. Kumar, H. L. Murray, R. G. Jenner, D. K. Gifford, D. A. Melton, R. Jaenisch, and R. A. Young.** 2005. Core transcriptional regulatory circuitry in human embryonic stem cells. Cell **122:**947–956.
3. **Burgess, S., G. Reim, W. Chen, N. Hopkins, and M. Brand.** 2002. The zebrafish spiel-ohne-grenzen (spg) gene encodes the POU domain protein Pou2 related to mammalian Oct4 and is essential for formation of the midbrain and hindbrain, and for pre-gastrula morphogenesis. Development **129:**905–916.
4. **Cai, X., C. H. Hagedorn, and B. R. Cullen.** 2004. Human microRNAs are processed from capped, polyadenylated transcripts that can also function as mRNAs. RNA **10:**1957–1966.
5. **Chew, J. L., Y. H. Loh, W. Zhang, X. Chen, W. L. Tam, L. S. Yeap, P. Li, Y. S. Ang, B. Lim, P. Robson, and H. H. Ng.** 2005. Reciprocal transcriptional regulation of Pou5f1 and Sox2 via the Oct4/Sox2 complex in embryonic stem cells. Mol. Cell. Biol. **25:**6031–6046.
6. **Conaco, C., S. Otto, J. J. Han, and G. Mandel.** 2006. Reciprocal actions of REST and a microRNA promote neuronal identity. Proc. Natl. Acad. Sci. USA **103:**2422–2427.
7. **Devereux, T. R., I. Horikawa, C. H. Anna, L. A. Annab, C. A. Afshari, and J. C. Barrett.** 1999. DNA methylation analysis of the promoter region of the human telomerase reverse transcriptase (hTERT) gene. Cancer Res. **59:** 6087–6090.
8. **Dignam, J. D., R. M. Lebovitz, and R. G. Roeder.** 1983. Accurate transcription initiation by RNA polymerase II in a soluble extract from isolated mammalian nuclei. Nucleic Acids Res. **11:**1475–1489.
9. **Fazi, F., A. Rosa, A. Fatica, V. Gelmetti, M. L. De Marchis, C. Nervi, and I. Bozzoni.** 2005. A minicircuitry comprised of microRNA-223 and transcription factors NFI-A and C/EBPalpha regulates human granulopoiesis. Cell **123:**819–831.
10. **Fluckiger, A. C., G. Marcy, M. Marchand, D. Negre, F. L. Cosset, S. Mitalipov, D. Wolf, P. Savatier, and C. Dehay.** 2006. Cell cycle features of primate embryonic stem cells. Stem Cells **24:**547–556.
11. **Fuhrmann, G., A. C. Chung, K. J. Jackson, G. Hummelke, A. Baniahmad, J. Sutter, I. Sylvester, H. R. Scholer, and A. J. Cooney.** 2001. Mouse germline restriction of Oct4 expression by germ cell nuclear factor. Dev. Cell **1:**377–387.
12. **Giraldez, A. J., R. M. Cinalli, M. E. Glasner, A. J. Enright, J. M. Thomson, S. Baskerville, S. M. Hammond, D. P. Bartel, and A. F. Schier.** 2005. MicroRNAs regulate brain morphogenesis in zebrafish. Science **308:**833–838.
13. **Giraldez, A. J., Y. Mishima, J. Rihel, R. J. Grocock, S. Van Dongen, K. Inoue, A. J. Enright, and A. F. Schier.** 2006. Zebrafish MiR-430 promotes deadenylation and clearance of maternal mRNAs. Science **312:**75–79.
14. **Hatfield, S. D., H. R. Shcherbata, K. A. Fischer, K. Nakahara, R. W. Carthew, and H. Ruohola-Baker.** 2005. Stem cell division is regulated by the microRNA pathway. Nature **435:**974–978.
15. **Houbaviy, H. B., M. F. Murray, and P. A. Sharp.** 2003. Embryonic stem cell-specific microRNAs. Dev. Cell **5:**351–358.

16. **Jirmanova, L., M. Afanassieff, S. Gobert-Gosse, S. Markossian, and P. Savatier.** 2002. Differential contributions of ERK and PI3-kinase to the regulation of cyclin D1 expression and to the control of the G1/S transition in mouse embryonic stem cells. Oncogene **21:**5515–5528.
17. **Kinyamu, H. K., and T. K. Archer.** 2003. Estrogen receptor-dependent proteasomal degradation of the glucocorticoid receptor is coupled to an increase in Mdm2 protein expression. Mol. Cell. Biol. **23:**5867–5881.
18. **Knuppel, R., P. Dietze, W. Lehnberg, K. Frech, and E. Wingender.** 1994. TRANSFAC retrieval program: a network model database of eukaryotic transcription regulating sequences and proteins. J. Comput. Biol. **1:**191–198.
19. **Lee, Y., M. Kim, J. Han, K. H. Yeom, S. Lee, S. H. Baek, and V. N. Kim.** 2004. MicroRNA genes are transcribed by RNA polymerase II. EMBO J. **23:**4051–4560.
20. **Lewis, B. P., C. B. Burge, and D. P. Bartel.** 2005. Conserved seed pairing, often flanked by adenosines, indicates that thousands of human genes are microRNA targets. Cell **120:**15–20.
21. **Lewis, B. P., I. H. Shih, M. W. Jones-Rhoades, D. P. Bartel, and C. B. Burge.** 2003. Prediction of mammalian microRNA targets. Cell **115:**787–798.
22. **Linsley, P. S., J. Schelter, J. Burchard, M. Kibukawa, M. M. Martin, S. R. Bartz, J. M. Johnson, J. M. Cummins, C. K. Raymond, H. Dai, N. Chau, M. Cleary, A. L. Jackson, M. Carleton, and L. Lim.** 2007. Transcripts targeted by the microRNA-16 family cooperatively regulate cell cycle progression. Mol. Cell. Biol. **27:**2240–2252.
23. **Llave, C., Z. Xie, K. D. Kasschau, and J. C. Carrington.** 2002. Cleavage of Scarecrow-like mRNA targets directed by a class of Arabidopsis miRNA. Science **297:**2053–2056.
24. **Loh, Y. H., Q. Wu, J. L. Chew, V. B. Vega, W. Zhang, X. Chen, G. Bourque, J. George, B. Leong, J. Liu, K. Y. Wong, K. W. Sung, C. W. Lee, X. D. Zhao, K. P. Chiu, L. Lipovich, V. A. Kuznetsov, P. Robson, L. W. Stanton, C. L. Wei, Y. Ruan, B. Lim, and H. H. Ng.** 2006. The Oct4 and Nanog transcription network regulates pluripotency in mouse embryonic stem cells. Nat. Genet. **38:**431–440.
25. **Miranda, K. C., T. Huynh, Y. Tay, Y. S. Ang, W. L. Tam, A. M. Thomson, B. Lim, and I. Rigoutsos.** 2006. A pattern-based method for the identification of MicroRNA binding sites and their corresponding heteroduplexes. Cell **126:**1203–1217.
26. **Mitsui, K., Y. Tokuzawa, H. Itoh, K. Segawa, M. Murakami, K. Takahashi, M. Maruyama, M. Maeda, and S. Yamanaka.** 2003. The homeoprotein Nanog is required for maintenance of pluripotency in mouse epiblast and ES cells. Cell **113:**631–642.
27. **Murchison, E. P., J. F. Partridge, O. H. Tam, S. Cheloufi, and G. J. Hannon.** 2005. Characterization of Dicer-deficient murine embryonic stem cells. Proc. Natl. Acad. Sci. USA **102:**12135–12140.
28. **Nichols, J., B. Zevnik, K. Anastassiadis, H. Niwa, D. Klewe-Nebenius, I. Chambers, H. Scholer, and A. Smith.** 1998. Formation of pluripotent stem cells in the mammalian embryo depends on the POU transcription factor Oct4. Cell **95:**379–391.
29. **Nishimoto, M., A. Fukushima, A. Okuda, and M. Muramatsu.** 1999. The gene for the embryonic stem cell coactivator UTF1 carries a regulatory element which selectively interacts with a complex composed of Oct-3/4 and Sox-2. Mol. Cell. Biol. **19:**5453–5465.
30. **Niwa, H., K. Yamamura, and J. Miyazaki.** 1991. Efficient selection for high-expression transfectants with a novel eukaryotic vector. Gene **108:**193–199.
31. **O'Donnell, K. A., E. A. Wentzel, K. I. Zeller, C. V. Dang, and J. T. Mendell.** 2005. c-Myc-regulated microRNAs modulate E2F1 expression. Nature **435:**839–843.
32. **Okumura-Nakanishi, S., M. Saito, H. Niwa, and F. Ishikawa.** 2005. Oct-3/4 and Sox2 regulate Oct-3/4 gene in embryonic stem cells. J. Biol. Chem. **280:**5307–5317.
33. **Quandt, K., K. Frech, H. Karas, E. Wingender, and T. Werner.** 1995. MatInd and MatInspector: new fast and versatile tools for detection of consensus matches in nucleotide sequence data. Nucleic Acids Res. **23:**4878–4884.
34. **Rao, P. K., R. M. Kumar, M. Farkhondeh, S. Baskerville, and H. F. Lodish.** 2006. Myogenic factors that regulate expression of muscle-specific microRNAs. Proc. Natl. Acad. Sci. USA **103:**8721–8726.
35. **Remenyi, A., K. Lins, L. J. Nissen, R. Reinbold, H. R. Scholer, and M. Wilmanns.** 2003. Crystal structure of a POU/HMG/DNA ternary complex suggests differential assembly of Oct4 and Sox2 on two enhancers. Genes Dev. **17:**2048–2059.
36. **Rodda, D. J., J. L. Chew, L. H. Lim, Y. H. Loh, B. Wang, H. H. Ng, and P. Robson.** 2005. Transcriptional regulation of nanog by OCT4 and SOX2. J. Biol. Chem. **280:**24731–24737.
37. **Savatier, P., S. Huang, L. Szekely, K. G. Wiman, and J. Samarut.** 1994. Contrasting patterns of retinoblastoma protein expression in mouse embryonic stem cells and embryonic fibroblasts. Oncogene **9:**809–818.
38. **Savatier, P., H. Lapillonne, L. A. van Grunsven, B. B. Rudkin, and J. Samarut.** 1996. Withdrawal of differentiation inhibitory activity/leukemia inhibitory factor up-regulates D-type cyclins and cyclin-dependent kinase inhibitors in mouse embryonic stem cells. Oncogene **12:**309–322.
39. **Suh, M. R., Y. Lee, J. Y. Kim, S. K. Kim, S. H. Moon, J. Y. Lee, K. Y. Cha, H. M. Chung, H. S. Yoon, S. Y. Moon, V. N. Kim, and K. S. Kim.** 2004. Human embryonic stem cells express a unique set of microRNAs. Dev. Biol. **270:**488–498.
40. **Takahashi, K., and S. Yamanaka.** 2006. Induction of pluripotent stem cells from mouse embryonic and adult fibroblast cultures by defined factors. Cell **126:**663–676.
41. **Tokuzawa, Y., E. Kaiho, M. Maruyama, K. Takahashi, K. Mitsui, M. Maeda, H. Niwa, and S. Yamanaka.** 2003. Fbx15 is a novel target of Oct3/4 but is dispensable for embryonic stem cell self-renewal and mouse development. Mol. Cell. Biol. **23:**2699–2708.
42. **Yuan, H., N. Corbi, C. Basilico, and L. Dailey.** 1995. Developmental-specific activity of the FGF-4 enhancer requires the synergistic action of Sox2 and Oct-3. Genes Dev. **9:**2635–2645.